



## Synthesis, Characterization and Anticancer Activity of Poly Acetal /PVP Ag, Au Nanocomposite in Treatment of Lung Cancer Cell Line

Dalia J. Hadi<sup>1</sup>  and Maha A. Younus<sup>2\*</sup> 

<sup>1,2</sup>Department of Chemistry, College of Education for Pure Science (Ibn Al-Haitham), University of Baghdad, Baghdad, Iraq.

\*Corresponding Author.

Received: 20 June 2023

Accepted: 21 August 2023

Published: 20 January 2025

[doi.org/ 10.30526/38.1.3607](https://doi.org/10.30526/38.1.3607)

### Abstract

In this research, poly acetal has been prepared from poly vinyl alcohol reaction with the para methyl benzaldehyde. The solution casting process was used to create the polymer blends of poly acetal and PVP. The aim of this study is to investigate the influence of the gold and silver nano particles on the anticancer activity of the prepared compounds. Using onion peel extract as a reducing agent, the gold nanoparticles (AuNPs) and silver nanoparticles (AgNPs) were created. Nanocomposite were prepared by solution casting by mixing poly acetal /PVP /Au, Ag nano particles with different ratios. The AuNPs and AgNPs were characterized through XRD analysis and FESEM microscopy. The poly acetal, polymer blends and nano composite were characterized by FTIR, FESEM, DSC and TGA. The FTIR has been used to analyze poly acetal, which confirms its production by displaying a new band of absorption at  $1105\text{ cm}^{-1}$  due to the (O-C-O). The thermal stability of the generated polymer blends and nanocomposites is confirmed by DSC and TGA; in comparison to blends, nanocomposites have demonstrated good performance in suppressing lung cancer cell lines.

**Keywords:** Anti-cancer cell line, PVP, polyacetal, nanocomposite.

### 1. Introduction

Renewability, sustainability, nontoxicity, and biodegradability are just a few of the many attributes that biopolymers, which are biodegradable polymers, possess. Additionally, they are inert, noncancerogenic, and no immunogenic (1). The non-halogenated aliphatic polymer polyvinyl alcohol (PVA) is a water-soluble polyhydroxy polymer with a two-dimensional hydrogen-bonded network sheet structure. Having both crystalline and amorphous phases, PVA is a semi-crystalline polymer (2). PVA is an excellent hydrophilic polymer because of its extremely adequate physicochemical properties, nontoxicity, and biocompatibility (3).



As a result of its compatible structure and hydrophilic properties, this polymer is frequently blended with other polymer compounds, including biopolymers and other polymers, to improve the mechanical properties of films in various industrial applications (4). Early transition metals can form polyoxometalates (POMs), macro anionic clusters in which an oxygen bridge connects the metal ions in their most extraordinary oxidation states. Because of their distinctive characteristics and reactivity, they have been investigated in various domains, including catalysis, material science, pharmaceutical research, medicine, and biosensors. POMs have garnered much attention in recent years in pharmaceutical research as potential therapeutic agents such as anti-cancer, antibacterial, and antiviral drugs. It appears that they have a remarkable probability of being considered as medications in the future due to their low cost of production, straightforward synthesis, ease of modification, and other notable properties (5). A synthetic polymer called polyvinylpyrrolidone (PVP) is renowned for being non-toxic, bio-inert, and hydrophilic, making it a promising candidate for use in pharmaceutical applications for drug administration (6). Its capacity to form complexes with several smaller molecules has allowed drug-conjugated polymeric matrices to increase drug bioavailability and sustained release (7). Because they integrated the synergistic features of many materials into a new composite with targeted performance by overcoming the shortcomings of the individual components, polymer blends are regarded as one of the most practicable approaches (8). Materials containing organized components with at least one dimension less than 100 nm are called nanomaterials. Thin films and surface coatings are examples of layers with just one dimension at the nanoscale (but are expanded in the other two dimensions) (9). Creating metallic nanoparticle colloidal solutions is one of the key fields of current science. Gold nanoparticles (NPs) and their uses are among the most researched materials in numerous fields, including optoelectronics and catalysis (10). Due to their potent antibacterial activity in both solution and components, silver NPs (Ag-NPs) among gold NPs must also be regarded as a highly significant and in-demand material for tissue engineering and antibacterial applications (11). Silver NPs are used in biotechnology, electronics, environmental research, medicine, and medical devices (12). Multi-phase materials called nanocomposites have at least one phase with diameters between 10 and 100 nm.

Nanocomposite materials have recently come to light as viable options to alleviate the shortcomings of many engineering materials. They are reportedly the 21<sup>st</sup> century's materials. Dispersed matrix and dispersed phase materials are two categories of nanocomposite materials (13). Cell growth that is aberrant and unchecked might be characterized as cancer. Through the blood or lymphatic system, cancer cells frequently metastasize to distant organs or spread into nearby tissue. Many tissues and organs are capable of developing cancerous cells. Despite improvements in early diagnosis and treatment, cancer remains a significant health issue that requires the greatest priority for research (14). Because dimensionality significantly affects material characteristics, including NPs increases nanocomposites' mechanical, thermal, optical, and antibacterial properties (15). The current study aims to prepare gold and silver nanocomposites from polyacetal and PVP to develop a new nanocomposite with desirable biomedical properties.

## 2. Materials and Methods

### 2.1. Preparation of polyacetal

To prepare polyacetal, 1 g of PVA was dissolved in 25 mL of dimethyl sulfoxide (DMSO) and stirred for 30 minutes at room temperature; 1 g of para methyl benzaldehyde was dissolved in 20 mL of absolute ethanol with 3 drops of concentrated  $\text{H}_2\text{SO}_4$  and stirred for 30 minutes at  $50^\circ\text{C}$  temperature. The mixture was heated for nine hours with reflux at a temperature of  $50^\circ\text{C}$  while being magnetically swirled. A few drops of (1N) NaOH solution were added to the resultant combination to lower the pH to 7. The product was filtered after cooling, and an oven at  $50^\circ\text{C}$  was used to dry it for 24 hours (16). The synthesis of polyacetal (PA) is shown in **Figure 1**.

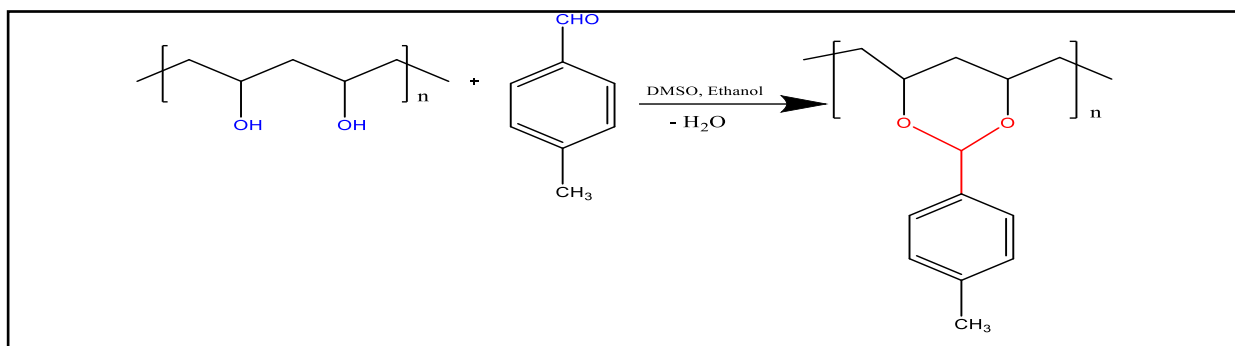


**Figure 1.** Synthesis of poly acetal.

### 2.2. Polymer blend preparation

Solution casting was used to create polymer blends, while dissolution was used to develop polyacetal solution. One gram of polyacetal was dissolved in one hundred milliliters of DMSO while stirred at 50 degrees Celsius. Five grams of PVP were dissolved in one hundred milliliters of water to create a five-weight percent solution of the polymer. The mixture solution was poured onto petri dishes and dried for 24 hours at  $50^\circ\text{C}$  in the oven. Blends of PA/PVP (25% PVP-75%PA, 50%PVP-50%PA) were created by combining various ratios (17).

### 2.3. Biosynthesis of gold and silver nanoparticles

To make a crude extract from onion leaves to make the onion peel extract, 10 g of leaf powder was mixed with 100 mL of deionized water. The mixture was heated to  $50^\circ\text{C}$  for two hours while being agitated, and the end product was filtered and dried in an oven at that temperature. To get onion peel extract (100 ppm), 0.01 g of powder product was dissolved in 100 milliliters of deionized water. Fresh onion peel extract was used as a stabilizing and reducing agent (18). To prepare  $\text{HAuCl}_4 \cdot 3\text{H}_2\text{O}$ ,  $\text{AgNO}_3$  Solutions, stock solutions were made by the following procedure: 1 g of gold chloride trihydrate ( $\text{HAuCl}_4 \cdot 3\text{H}_2\text{O}$ ) was dissolved in 100 mL of deionized water. Then, 2 mL of the stock solution was taken, and the remaining 100 mL was finished using successive dilution procedures to achieve (100 ppm). A combination of (0.016g) of  $\text{AgNO}_3$  was created with (100 ppm) of deionized water in 100 mL  $\text{AgNO}_3$ . After that, 10 mL of aqueous gold chloride solution, 3 mL of aqueous onion peel extract, and silver nitrate were added in that order, and the combined liquid was then stirred for 10 minutes at  $25^\circ\text{C}$ . The color of the gold changed from yellow to purple to show the development of AuNPs, while the color of the silver changed

from colorless to brown to show the synthesis of AgNPs. The precipitate is removed, gathered, and thinned with deionized water during the nanoparticle separation process after being separated from the filtrate by a centrifuge (10000 ppm) (19).

#### **2.4. Gold and silver nanocomposites preparation**

The nanocomposite film was created by adding 15 mL of poly acetal, 5 mL of PVP, and 20 mL of concentrations (100 ppm) of AuNPs and AgNPs in the correct order, and the mixture was stirred for 2 hours. The mixture was then put into Petri plates and kept at 50 ° C for 24 hours.

#### **2.5. Anticancer activity**

##### **2.5.1. Cell cultures**

The A1549 cells were kept alive in RPMI-1640 media containing 10% fetal bovine serum, 100 Units/mL penicillin, and 100 g/mL streptomycin. They were passaged using trypsin-EDTA, reseeded at 80% confluence, and grown at 37 °C twice weekly (20,21).

##### **2.5.2. Cytotoxicity assays**

The cytotoxic effects of polymer mixes and nanocomposites were evaluated using 96-well plates and the MTT test (22,23). One hundred four cells from each cell line were planted in each well. Cells were treated to nanocomposites in concentrations after 24 hours or after forming a confluent monolayer. Cell viability was assessed 48 hours after the treatment by removing the medium, adding 28 L of an MTT solution containing 2 mg/mL, and incubating the cells for 2.5 h at 37 °C. Following removal of the MTT solution, the residual crystals in the wells were solubilized by adding 130 L of DMSO (dimethyl sulphoxide), which was then incubated for 15 minutes at 37 °C while being shaken (24). The absorbency was measured in triplicate during the experiment using a microplate reader set to 492 nm. The following calculation was used to compute the percentage of cytotoxicity or the rate at which cell growth was inhibited (25,26). The formula for calculating the inhibition rate is  $A-B/A*100$ , where A represents the optical density of the control, and B means that of the samples (27). An inverted microscope was used to examine the morphology of the cells after they had been seeded into 24-well micro-titration plates at a density of  $1 \times 10^5$  cells  $mL^{-1}$  and cultured for 24 hours at 37 °C. After that, polymer mixtures and nanocomposites were applied to cells for 24 hours. The plates were dyed with crystal violet dye after the exposure period, and they were then heated to 37 °C for a further 10-15 minutes (25). Mild washing with tap water is needed to remove the color from the area altogether. The cells were examined using an inverted microscope with 100x magnification, and a digital camera was attached to the microscope to capture images (28 -30).

##### **2.5.3. Statistical analysis**

The data collected in Graph Pad Prism 6 were statistically analyzed using an unpaired t-test (31). The average and standard deviation of three measurements were used to present the results (32).

### **3. Results and Discussion**

#### **3.1. Characterization of AuNPs and AgNPs**

Utilizing X-ray Powder Diffraction (XRD) (Malvern Panalytical) and SEM microscopy (TESCAN Czech Republic), the produced AuNPs and AgNPs were analyzed.

### 3.1.2. Scanning electron microscopy

The SEM microscopy, an analytical technique, may identify the typical size and shape of NPs in the test material (33). The surface of the AuNPs and AgNPs made from onion peels utilizing green synthesis is shown in **Figure 2**. The SEM image showed the shape of AuNPs with a diameter of 41.61 nm and silver NPs with a diameter of 29.45 nm. The surface morphology changes for the prepared polyacetal, PA/PVP polymer blend, and Au, Ag nanocomposites were studied using the SEM technique, as shown in **Figure 3**.

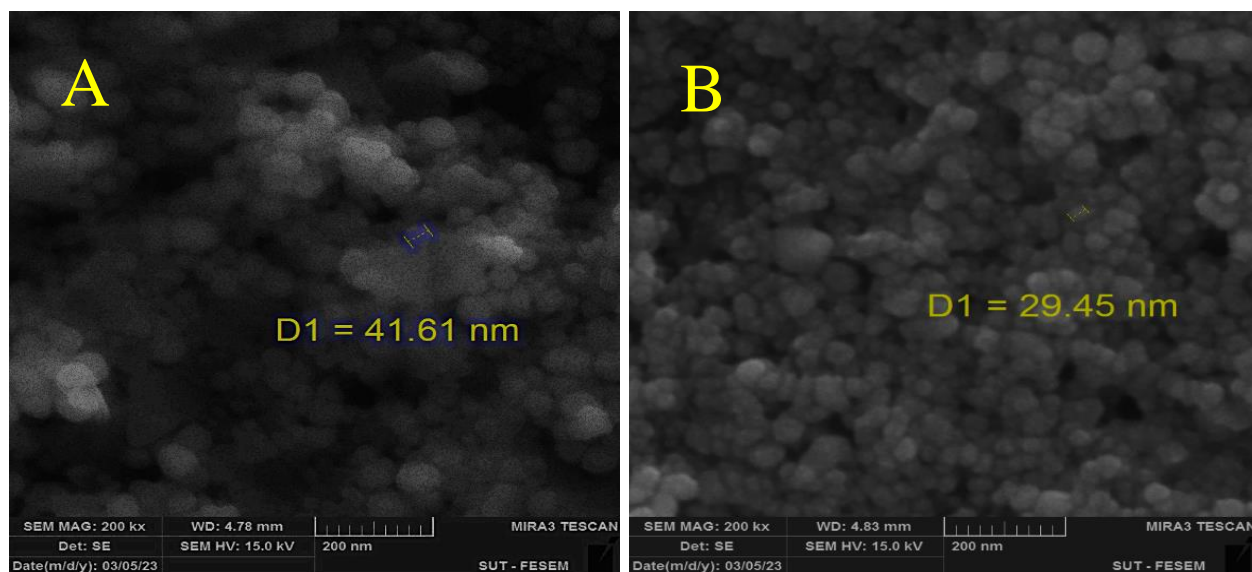


**Figure 2.** Scanning electron microscopy of (A- AuNPs) and (B- AgNPs).

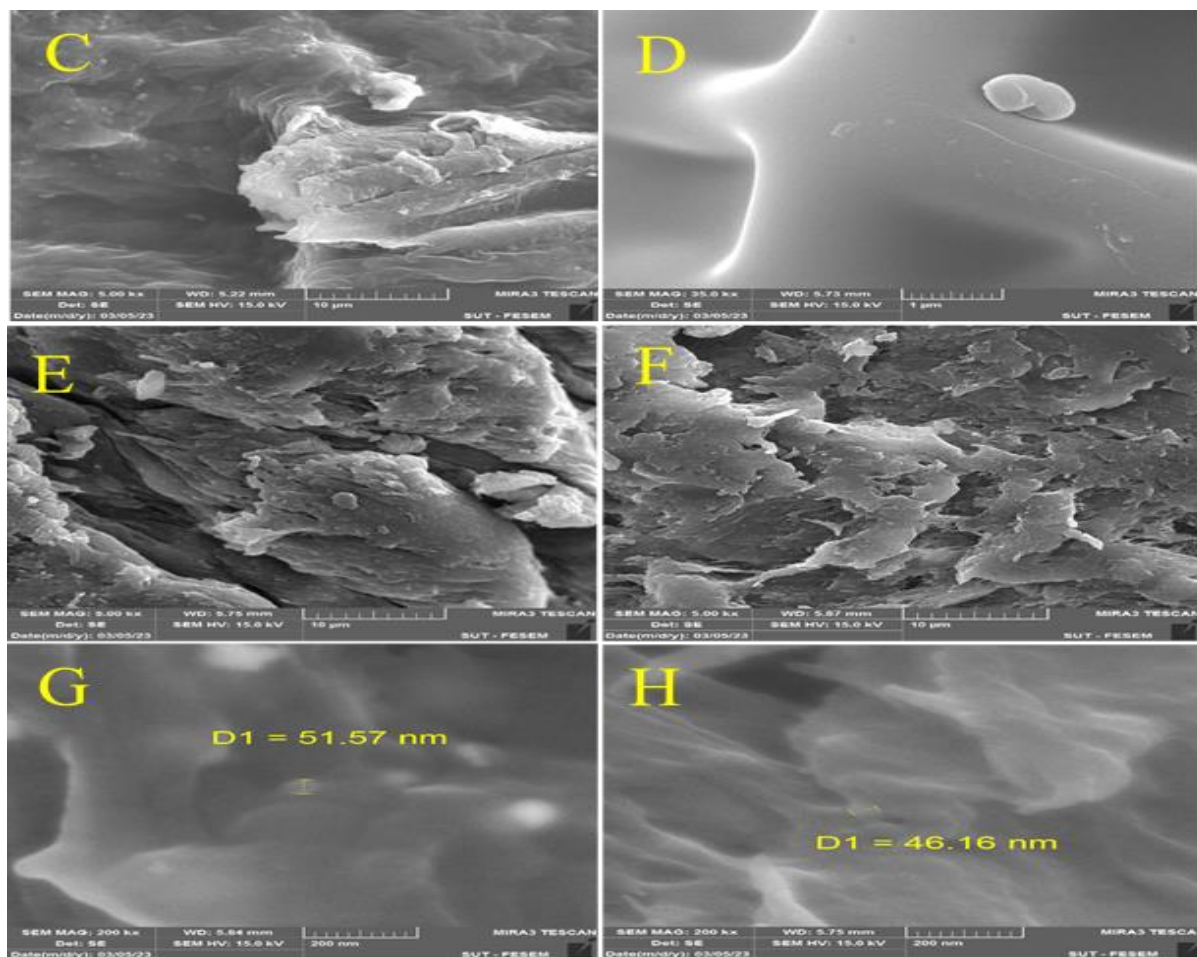


**Figure 3.** Scanning electron microscopy of (A- AuNPs) and (B- AgNPs) (C- polyacetal), (D- PVP), (E- polymer blend 1), (F- polymer blend 2), (G Nanocomposite (PA/ PVP -AuNPs), (H (PA/ PVP-AgNPs).

### 3.1.3. Analysis of X-ray diffraction (XRD)

AgNPs and AuNPs that had been synthesized were evaluated for their crystallinity using X-ray diffraction (XRD) analysis. **Figures 4 A** and **B** display the XRD results of the AuNPs and AgNPs that were created. The fact that dried AuNPs exhibited peaks at  $38^\circ$ ,  $44^\circ$ , and  $49^\circ$  that matched Bragg's planes (111), (200), and (220), respectively, demonstrated that the created AuNPs had a face-centered cubic structure. By (JCPDS 04-0784), dried AgNPs showed a 2theta degree ranging from 10 to 80 (34). According to (JCPDS 04-0783), the peak for AgNPs produced at 2theta values  $38^\circ$ ,  $49^\circ$ , and  $69^\circ$  corresponds to Bragg's reflection (200), (200), respectively (35).

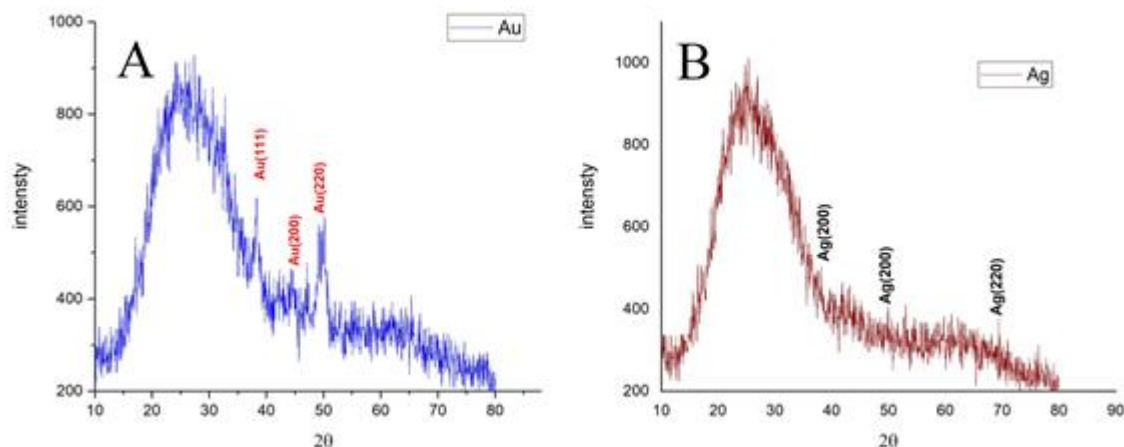


**Figure 4.** The XRD patterns of (A-AuNPs) and (B- AgNPs).

### 3.2. Characterization of polyacetal, PVP, polymer blend FT-IR Analysis

**Figure 5-A** shows the polyacetal FT-IR spectrum, which is allocated as follows: The broadband is  $(3389) \text{ cm}^{-1}$  for the (OH stretching vibration),  $2916 \text{ cm}^{-1}$  for the (C-H symmetric stretch),  $1606 \text{ cm}^{-1}$ , and  $1434 \text{ cm}^{-1}$  for the (C=C),  $1105 \text{ cm}^{-1}$  for the (C-O-C bending vibration), and  $950 \text{ cm}^{-1}$  for the (C-H are stretching vibration). A peak in the FTIR spectrum of PVP **Figure 5-B** at  $3423 \text{ cm}^{-1}$  suggests O-H stretching. Peaks at  $2951$  and  $1646 \text{ cm}^{-1}$ , respectively, demonstrated the occurrence of asymmetric stretching of  $\text{CH}_2$  and C-O. The C-H bending and  $\text{CH}_2$  wagging were seen at  $1425$  and  $1278 \text{ cm}^{-1}$  for the pyridine ring, respectively. The  $\text{CH}_2$  rock and the N-C=O bending were recognized as the peaks at  $1016$  and  $567 \text{ cm}^{-1}$  (36). **Figure 5-C** shows the created polymer mix. As a result of the hydroxyl group's (OH) of PVP's stretching vibration, C displayed a wide band at  $3407 \text{ cm}^{-1}$ . The band at about  $1017 \text{ cm}^{-1}$  denotes the presence of a hydroxyl group (OH), while a band at approximately  $1458 \text{ cm}^{-1}$  is attributed to the pyridine ring (C=N) (37).

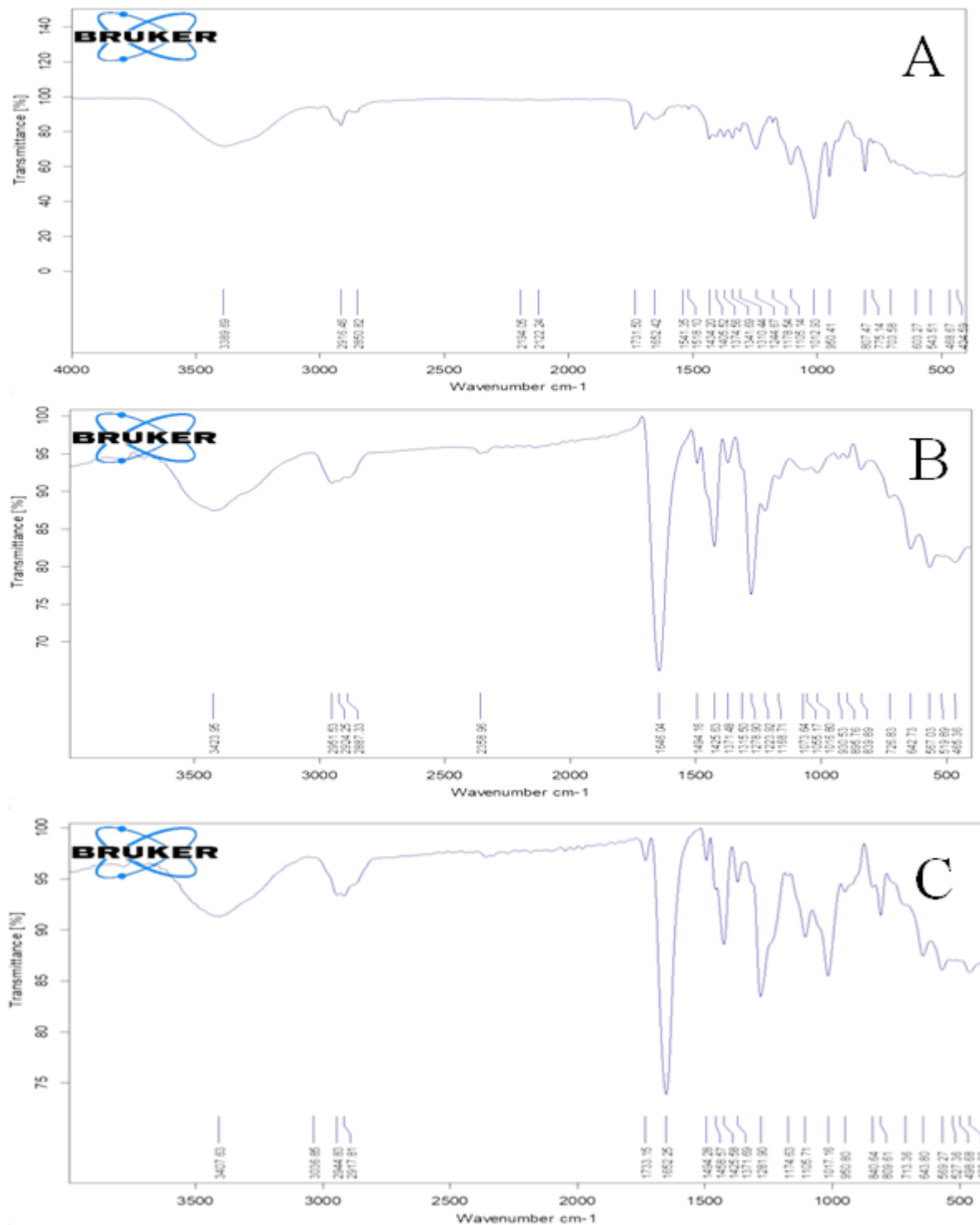


Figure 5. The FTIR spectrum (A-polyacetal), (B-PVP), C- polymer blend.

### 3.3. Thermal analysis (TGA, DSC)

At temperatures ranging from 25°C to 1000°C at a constant rate of 10°C per minute, the thermogravimetric analysis and differential scanning calorimeter (TGA, DSC) have been



utilized to study PVA, PVP, Polyacetal, PA/PVP polymer blend, and PA/PVP Au, Ag nanocomposites. Figure 6 shows the TGA curve of a PA/PVP polymer mix. A- showed a sequence of mass loss in four phases, the first of which had a mass loss of volatile chemicals (-8.058%). The second stage saw an estimated weight loss of (-5.523%), the third stage saw an approximate weight loss of (-73.34%), and the fourth stage saw an approximate weight loss of (-11.41%) (38). **Figure 6** shows a DSC curve. A's Tg for the PA/PVP polymer mix was (91.83°C) (39). Also, **Figure 6** shows the TGA curve of the nanocomposite PA/PVP-Ag. B- showed a sequence of mass loss in four phases, the first of which had a mass loss of volatile chemicals (-12.05%). The second stage had an average weight loss of (-6.76%), the third stage saw an average weight loss of (-48.24%), and the fourth stage saw an average weight loss of (-31.44%). The nanocomposite PA/PVP-Ag in **Figure 6-C**. DSC curve has a Tg of 100. 37°C. Peak concerning the polymer melting Tm at (460.49 °C). The PA/PVP-Au nanocomposite's TGA curve, shown in Figure 6-C, showed four phases of a sequence mass loss, the first of which saw a mass loss of volatile chemicals of (-8.648%). The second stage saw an estimated weight loss of (-5.000%), the third stage saw an approximate weight loss of (-64.03%), and the fourth stage saw an approximate weight loss of (-21.14%). The PA/PVP-Au nanocomposite's DSC curve in **Figure 6-C** displayed a Tg of (131.72°C). Peak concerning the polymer melting Tm at (468.72°C). All temperatures have been somewhat raised, demonstrating that the gold and silver's polymer blending and coordination bonding impact thermal stability. It has also been noted that the blend film only exhibits one Tg on its thermogram. This shows that the PA and PVP polymers are properly mixed, and hydrogen bonding interactions are present in the blend. These results suggest that Nano-Au & Ag can enhance the thermal stability of nanocomposites at such an incredibly low concentration, as illustrated in **Figure 6**.

### 3.4. Anticancer cell line

Blend, nanocomposites' cytotoxic impact on cancer cells was investigated. To evaluate the blend's anticancer effectiveness, nanocomposites were tested for their ability to inhibit the development of the lung cancer cell line A1549. The findings of this study showed that blend. As shown in **Figures 8** and **9**. Nanocomposites were exhibited against human cancer cell lines. Avery has a significant cytotoxic impact. The results demonstrate that blends and nanocomposites can prevent cell line growth and that this effect is concentration-dependent. The NPs direct their attention toward the tumor cells through aggregation and trapping. Another characteristic of the process is the retention and penetration impact that abnormal lymphatic flow and angiogenic vessels have on malignant cells; as a result, compared to normal cells, these NPs accumulate more or more specifically inside malignant cells. The findings indicated that nanocomposites have more inhibitors than a mix. The results showed that A1549 cells were cytotoxic, with IC50 values of 38.55 µg/mL for A, 22.59 µg/mL for B, and 27.87 µg/mL for C, and 42.06 µg/mL for D, and 24.26 µg/for E, and 30.92 µg/mL for F (40). As shown in **Figure 7**.

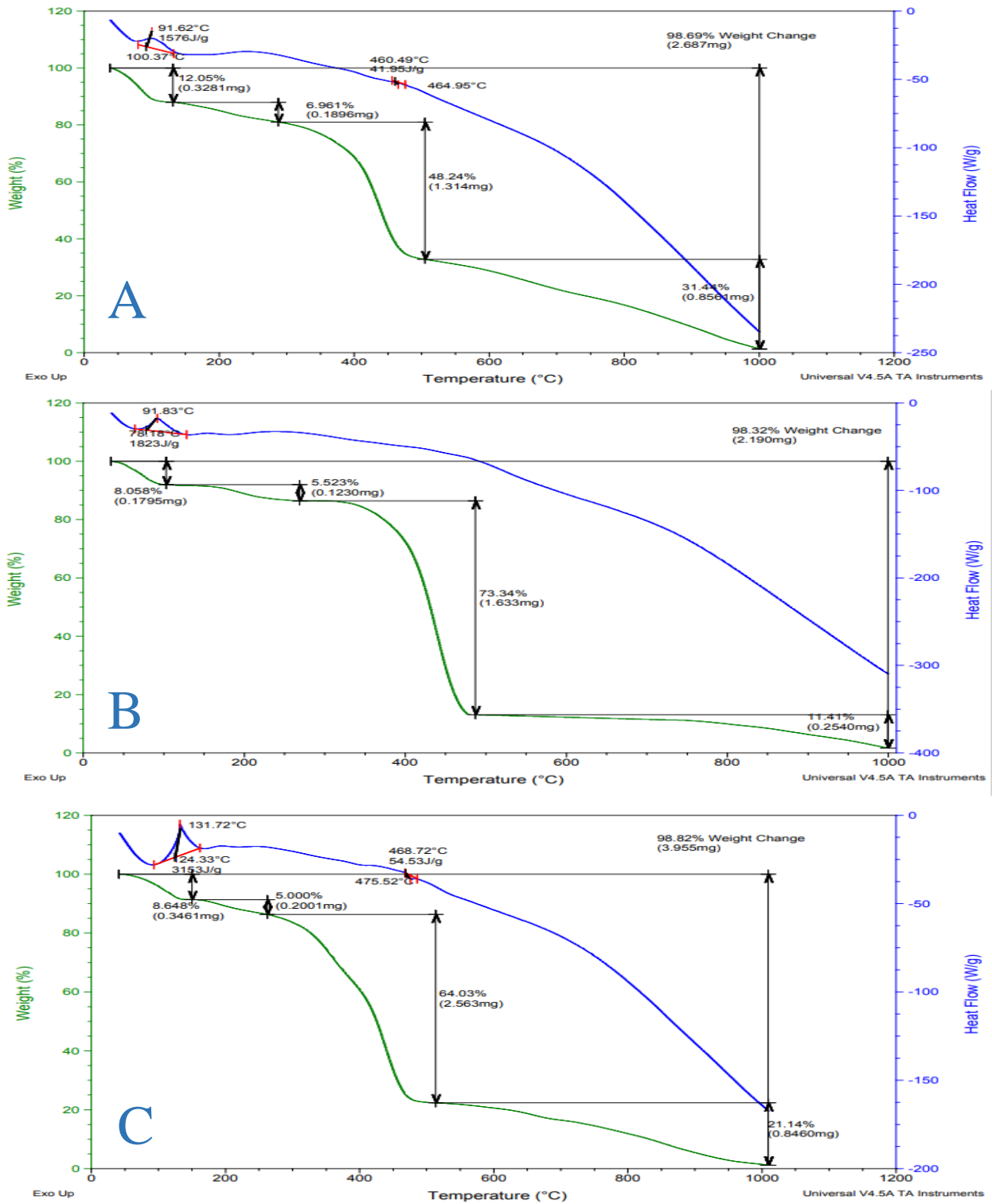


**Figure 6.** Thermal analysis (TGA, DSC), (A- Polymer blend), (B-Nanocomposite (PA / PVP -AgNPs)), (C- nanocomposite (PA/ PVP -AuNPs)).

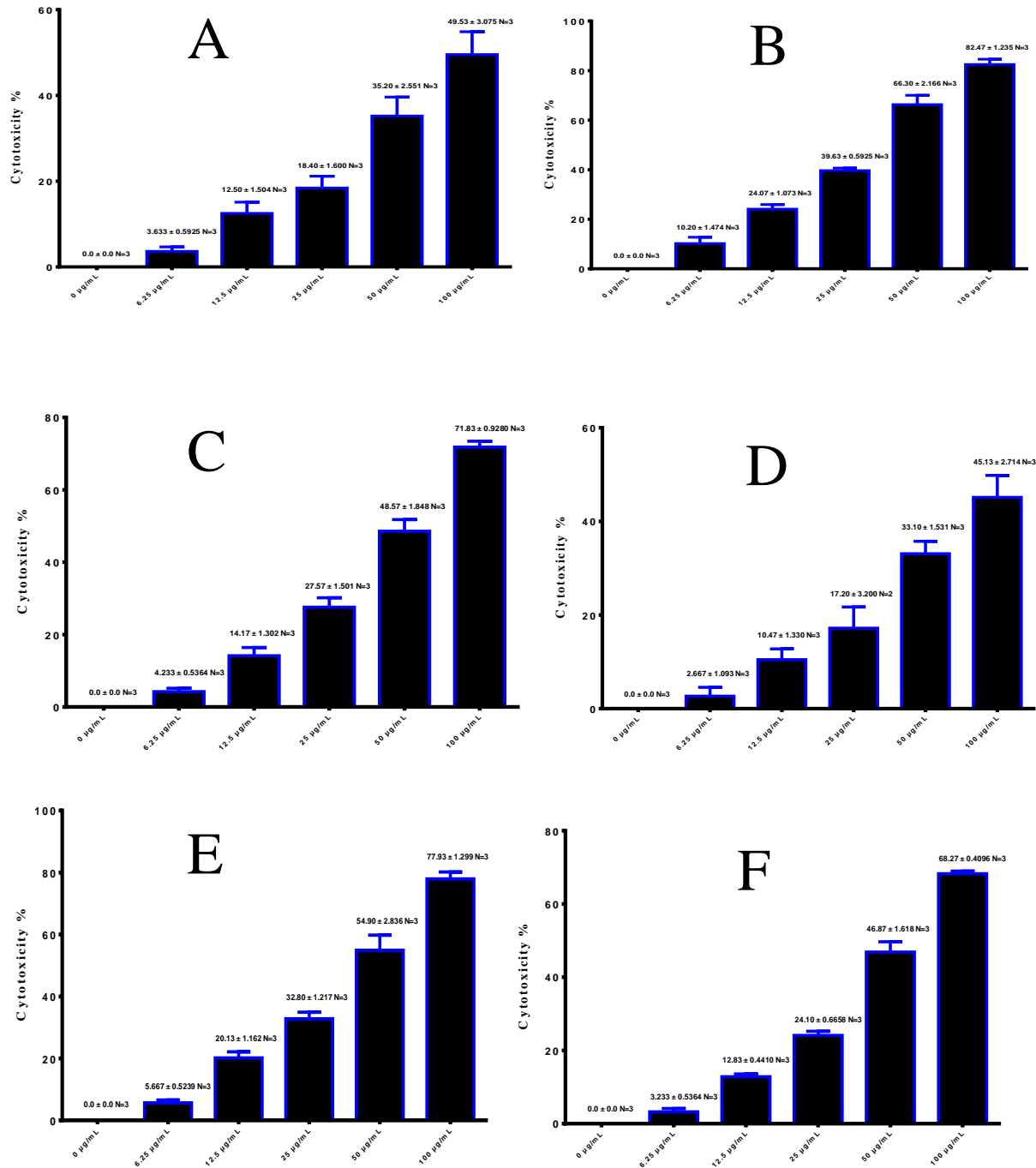


**Figure 7.** Effect of mixtures and nanocomposite materials (gold, silver) on cells A- Polymer blend1 A1549 cells. B- Nanocomposite PA/ PVP -AuNPs A1549 undergo morphological alterations after being treated with nanocomposite (Gold 100 ppm). C- Nanocomposite (PA/ PVP -AgNPs) A1549, D- Polymer blend2 A1549 cells. E- Nanocomposite PA/ PVP -AuNPs A1549 undergo morphological alterations after being treated with Nanocomposite (Gold 100 ppm) F- Nanocomposite (PA/ PVP-AgNPs) A1549 cells undergo morphological alterations after being treated with Nanocomposite (Silver 100 ppm). cells undergo morphological alterations after being treated with nanocomposite (Silver 100 ppm).

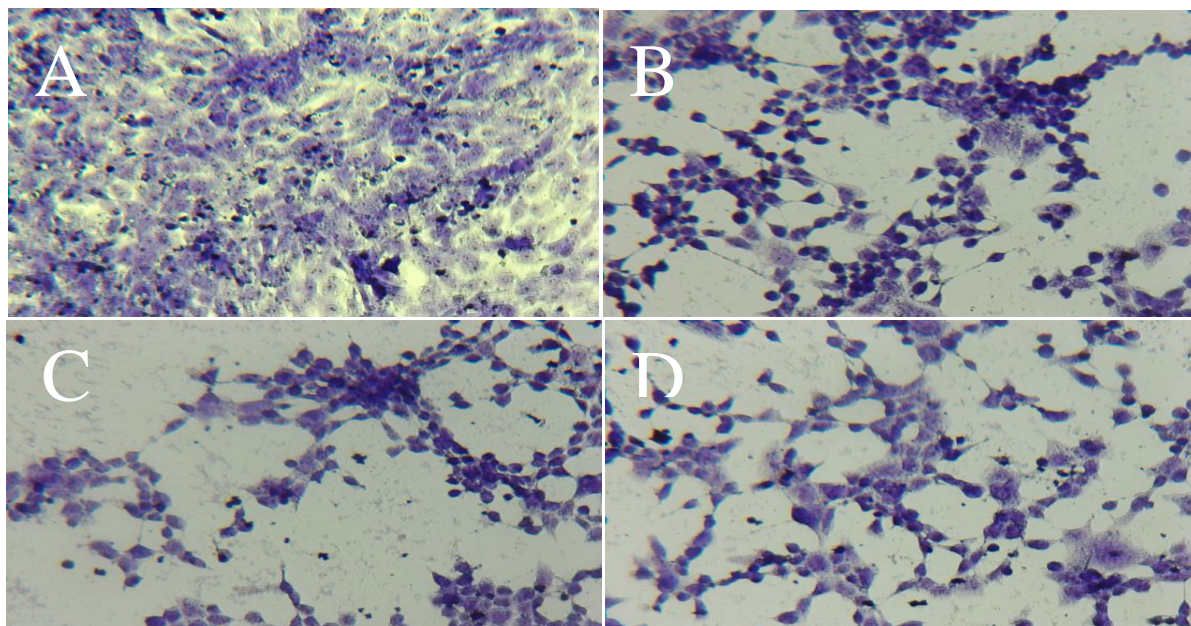


**Figure 8.** The A1549 cell morphology following treatment with A- Control ,B- Polymer blend1, C- Nanocomposite PA/ PVP -AuNPs, D- Nanocomposite (PA/ PVP -AgNPs).

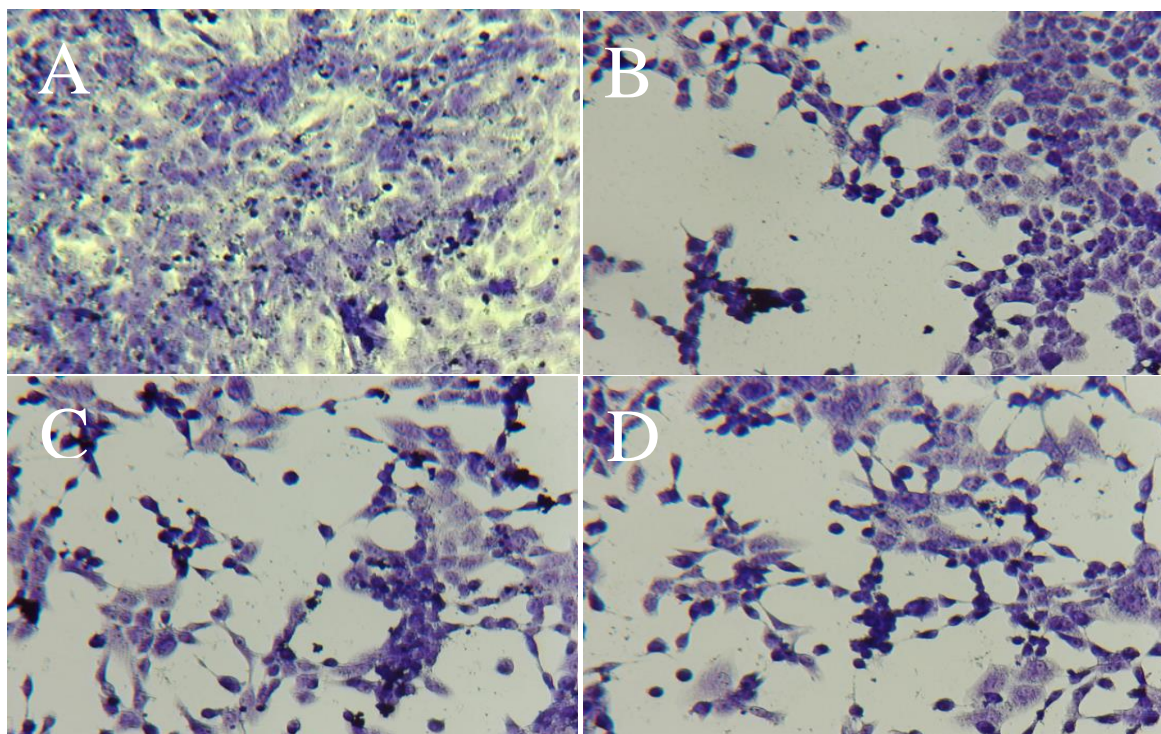


**Figure 9.** The A1549 cell morphology following treatment with A- Control B- Polymer blend2, C- Nanocomposite PA/ PVP -AuNPs, D- Nanocomposite (PA/ PVP -AgNPs).

#### 4. Conclusion

Polyacetal PA, PA/PVP polymer blends were prepared, and PA/PVP-Au, Ag nanocomposites. Onion peels were utilized as a reducing and stabilizing ingredient while creating gold and silver NPs. The crystallinity of these synthesized NPs was evaluated using XRD measurements. AuNPs and AgNPs were both face-centered cubic particles. Due to the presence of AuNPs and AgNPs, which increase activity toward the A1549 lung cancer cell line, nanocomposites have demonstrated more anticancer activity than polymer blends.

#### Acknowledgement

The authors thank the Department of Chemistry at the College of Education for Pure Sciences (Ibn Al-Haitham) for conducting this study in its laboratories.

#### Conflict of Interest

There is no conflict of interest.

#### Funding

There is no funding for the article.

#### Ethical Clearance

This work has been approved by the Scientific Committee at the University of Baghdad/ College of Education for Pure Science (Ibn Al-Haitham).

#### References

1. Ponnamma D, Sadasivuni KK, AlMaadeed MA. Biopolymer composites in electronics. Elsevier. 2017:1-12. <https://doi.org/10.1016/B978-0-12-809261-3.00001-2>
2. Samir AH, Saeed RS, Matty FS. Synthesis and study of modified polyvinyl alcohol containing amino acid moieties as anticancer agent. Orient J Chem. 2018; 34(1):286. <http://dx.doi.org/10.13005/ojc/340131>
3. Talib E N, Younus MA. Preparation, characterization and antimicrobial activity of chitosan schiff base/polyvinyl alcohol nanocomposite. JGPT 2019; 11(9), 87-92. <https://doi.org/10.21123/bsj.2023.7911>
4. Limpan N, Prodpran T, Benjakul S, Prasarnpran S. Influences of degree of hydrolysis and molecular weight of poly (vinyl alcohol)(PVA) on properties of fish myofibrillar protein/PVA blend films. Food hydrocoll. 2012; 29(1):226-233. <https://doi.org/10.1016/j.foodhyd.2012.03.007>
5. Hosseini M S, Haghjooy Javanmard S, Dana N, Rafiee L, Rostami M. Novel tocopherol succinate-polyoxomolybdate bioconjugate as potential anti-cancer agent. J Inorg Organomet Polym Mater. 2021; 31(7):3183-3195. <https://doi.org/10.21203/rs.3.rs-214396/v1>
6. Kumar G P, Phani A R, Prasad RG, Sanganal JS, Manali N, Gupta R, Raju DB. Polyvinylpyrrolidone oral films of enrofloxacin: film characterization and drug release. Int J Pharm. 2014; 471(1-2):146-152. <https://doi.org/10.1016/j.ijpharm.2014.05.033>
7. Hasan A, Waibhaw G, Tiwari S, Dharmalingam K, Shukla I, Pandey LM. Fabrication and characterization of chitosan, polyvinylpyrrolidone, and cellulose nanowhiskers nanocomposite films for wound healing drug delivery application. J Biomed Mater Res Part A. 2017; 105(9):2391-2404.

<https://doi.org/10.1002/jbm.a.36097>

8. Yong WF, Zhang H. Recent advances in polymer blend membranes for gas separation and pervaporation. *Prog Mater Sci.* 2021; 116:100713. <https://doi.org/10.1016/j.pmatsci.2020.100713>
9. Subramani K, Mehta M. Nanodiagnosics in microbiology and dentistry. In *Emerging nanotechnologies in dentistry*. William Andrew Publishing. 2018: 391-419. <https://doi.org/10.1016/B978-0-12-812291-4.00019-4>
10. Zhou J, Ralston J, Sedev R, Beattie DA. Functionalized gold nanoparticles: synthesis, structure and colloid stability. *J Colloid Interface Sci.* 2009; 331(2):251-262. <https://doi.org/10.1016/j.jcis.2008.12.002>
11. Naidu K S B, Adam J K, Govender P. Biomedical applications and toxicity of nanosilver: a review. *Medical Technology SA.* 2015; 29(2):13-19.
12. Slepíčka P, Slepíčková K N, Siegel J, Kolská Z, Švorčík V. Methods of gold and silver nanoparticles preparation. *Mater.* 2019; 13(1):1. <https://doi.org/10.3390/ma13010001>
13. Pandey N, Shukla SK, Singh NB. Water purification by polymer nanocomposites: an overview. *Nanocomposites.* 2017; 3(2):47-66. <https://doi.org/10.1080/20550324.2017.1329983>
14. Kharman-Biz A. Potential novel molecular targets for breast cancer diagnosis and treatment, Doctoral dissertation, Stockholm, Karolinska Institute, 2016.
15. Al-dabbag BM, Kadhim HJ. Nano composites of PAM reinforced with Al<sub>2</sub>O<sub>3</sub>. *Baghdad Sci J.* 2023; 20(6):2300-2306. <https://doi.org/10.21123/bsj.2023.7353>
16. Iqbal DN, Tariq M, Khan S M, Gull N, Iqbal SS, Aziz A, Iqbal M. Synthesis and characterization of chitosan and guar gum based ternary blends with polyvinyl alcohol. *Int J Biol Macromol.* 2020; 143: 546-554. <https://doi.org/10.1016/j.ijbiomac.2019.12.043>
17. Younus MA, Ali MU. Synthesis and antibacterial activity of PEG polycyclic acetal metal complex/PVA polymer blend film. *IHJPAS.* 2020; 33(3):44-54. <https://doi.org/10.30526/33.3.2472>
18. Younus MA, Abdallaha BF. Synthesis, characterization and anticancer activity of chitosan schiff base/PVP gold nano composite in treating esophageal cancer cell line. *Baghdad Sci J.* 2024; 21(1): 95-106 <https://doi.org/10.21123/bsj.2023.7911>
19. Abdallaha BF, Younus MA, Ibraheem IJ. Preparation, characterization, antimicrobial and antitumor activity of chitosan schiff base/PVA/PVP Au, Ag nanocomposite in treatment of breast cancer cell line. *Nanomed Res J.* 2021; 6(4):369-384. <https://doi.org/10.22034/nmrj.2021.04.007>
20. Al-Ziaydi AG, Al-Shammari AM, Hamzah MI, Jabir MS. Hexokinase inhibition using D-mannoheptulose enhances oncolytic newcastle disease virus-mediated killing of breast cancer cells. *Cancer Cell Int.* 2020; 20(1):1-10. <https://doi.org/10.1186/s12935-020-01514-2>
21. Al-Ziaydi AG, Hamzah MI, Al-Shammari AM, Kadhim HS, Jabir MS. The anti-proliferative activity of D-mannoheptulose against breast cancer cell line through glycolysis inhibition. *AIP Conf Proc.* 2020; 2307(1):020023. <https://doi.org/10.1063/5.0032958>
22. Mahmood RI, Kadhim AA, Ibraheem S, Albukhaty S, Mohammed-Salih HS, Abbas RH, Al-Karagoly H. Biosynthesis of copper oxide nanoparticles mediated *annona muricata* as cytotoxic and apoptosis inducer factor in breast cancer cell lines. *Sci Rep.* 2022; 12(1):1-10. <https://doi.org/10.1038/s41598-022-20360-y>
23. Al-Ziaydi AG, Al-Shammari AM, Hamzah MI, Kadhim HS, Jabir MS. Newcastle disease virus suppress glycolysis pathway and induce breast cancer cells death. *VirusDisease* 2020; 1-8. <https://doi.org/10.1007%2Fs13337-020-00612-z>
24. Jasim AJ, Sulaiman GM, Ay H, Mohammed SA, Mohammed HA, Jabir MS, Khan RA. Preliminary

- trials of the gold nanoparticles conjugated chrysin: An assessment of anti-oxidant, anti-microbial, and in vitro cytotoxic activities of a nanoformulated flavonoid. *Nanotechnol Rev.* 2022; 11(1):2726-2741. <https://doi.org/10.1515/ntrev-2022-0153>
25. Al-Musawi S, Albukhaty S, Al-Karagoly H, Sulaiman GM, Jabir MS, Naderi-Manesh H. Dextran-coated superparamagnetic nanoparticles modified with folate for targeted drug delivery of camptothecin. *Adv Nat Sci.: Nanosci.* 2020; 11(4):045009. [https://ui.adsabs.harvard.edu/link\\_gateway/2020ANSNN.11d5009A/doi:10.1088/2043-6254/abc75b](https://ui.adsabs.harvard.edu/link_gateway/2020ANSNN.11d5009A/doi:10.1088/2043-6254/abc75b)
  26. Al-Shammari AM, Al-Saadi H, Al-Shammari SM, Jabir MS. Galangin enhances gold nanoparticles as anti-tumor agents against ovarian cancer cells. *AIP Conf Proc.* 2020; 2213(1):020206. <https://doi.org/10.1063/5.0000162>
  27. Jawad M, Öztürk K, Jabir MS. TNF- $\alpha$  loaded on gold nanoparticles as promising drug delivery system against proliferation of breast cancer cells. *Mater. Today Proc.* 2021; 42:3057-3061. <https://doi.org/10.1016/j.matpr.2020.12.836>
  28. Abbas ZS, Sulaiman GM, Jabir MS, Mohammed SA, Khan RA, Mohammed HA, Al-Subaiyel A. galangin/ $\beta$ -cyclodextrin inclusion complex as a drug-delivery system for improved solubility and biocompatibility in breast cancer treatment. *Molecules* 2022; 27(14):4521. <https://doi.org/10.3390/molecules27144521>
  29. Ibrahim AA, Kareem MM, Al-Noor TH, Al-Muhimeed T, AlObaid AA, Albukhaty S, Sahib UI. Pt (II)-Thiocarbohydrazone complex as cytotoxic agent and apoptosis inducer in Caov-3 and HT-29 cells through the P53 and caspase-8 pathways. *Pharmaceuticals* 2021; 14(6):509. <https://doi.org/10.3390/ph14060509>
  30. Sameen AM, Jabir MS, Al-Ani MQ. Therapeutic combination of gold nanoparticles and LPS as cytotoxic and apoptosis inducer in breast cancer cells. *AIP Conf Proc.* 2020; 2213(1):020215. <https://doi.org/10.1063/5.0000161>
  31. Bahjat HH, Ismail RA, Sulaiman GM, Jabir MS. Magnetic field-assisted laser ablation of titanium dioxide nanoparticles in water for anti-bacterial applications. *J Inorg Organomet Polym Mater.* 2021:1-8. <https://doi.org/10.21203/rs.3.rs-176836/v1>
  32. Jihad MA, Noori FTM, Jabir MS, Albukhaty S, AlMalki FA, Alyamani AA. Polyethylene glycol functionalized graphene oxide nanoparticles loaded with nigella sativa extract: A smart antibacterial therapeutic drug delivery system. *Molecules.* 2021; 26:3067. <https://doi.org/10.3390/molecules26113067>
  33. Soshnikova V, Kim YJ, Singh,P, Huo Y, Markus J, Ahn S, Yang DC. Cardamom fruits as a green resource for facile synthesis of gold and silver nanoparticles and their biological applications. *Artif Cells Nanomed Biotechnol.* 2018; 46(1):108-117. <https://doi.org/10.1080/21691401.2017.1296849>
  34. Rajeshkumar S. Anticancer activity of eco-friendly gold nanoparticles against lung and liver cancer cells. *JGEB.* 2016; 14(1):195-202. <https://doi.org/10.1016/j.jgeb.2016.05.007>
  35. Pokrowiecki R, Wojnarowicz J, Zareba T, Koltsov I, Lojkowski W, Tyski S, Zawadzki P. Nanoparticles and human saliva: A step towards drug delivery systems for dental and craniofacial biomaterials. *Int J Nanomedicine.* 2019;14:9235. <https://doi.org/10.2147/IJN.S221608>
  36. Rahma A, Munir MM, Khairurrijal Prasetyo A, Suendo V, Rachmawati H. Intermolecular interactions and the release pattern of electrospun curcumin-polyvinylpyrrolidone) fiber. *Biol. Pharm. Bull.* 2016; 39(2):163-173. <https://doi.org/10.1248/bpb.b15-00391>
  37. Pokrowiecki R, Wojnarowicz J, Zareba T, Koltsov I, Lojkowski W, Tyski S, Zawadzki P. Nanoparticles and human saliva: a step towards drug delivery systems for dental and craniofacial

- biomaterials. Int J Nanomedicine. 2019: 9235-9257. <https://doi.org/10.2147/IJN.S221608>
38. Abass SM, Wahab MA, Mohammed HS, Hashim AA. Study of rheological and mechanical properties of bitumen blended with two alpha phases of polyamide. AIP Conf Proc. 2021; 2372(1): 130006. <https://doi.org/10.1063/5.0065985>
39. Ahmed BJ, Saleem MH, Matty FS. Synthesis and study of the antimicrobial activity of modified polyvinyl alcohol films incorporated with silver nanoparticles. Baghdad Sci J. 2023; 20(5):1643-1653. <https://doi.org/10.21123/bsj.2023.7471>
40. Shah A, Ashames AA, Buabeid MA, Murtaza G. Synthesis, in vitro characterization and antibacterial efficacy of moxifloxacin-loaded chitosan-pullulan-silver-nanocomposite films. JDDT. 2020; 55:101366. <https://doi.org/10.1016/j.jddst.2019.101366>